Logistic Chaos-Based Wild Horse Optimization for Enhanced Color Image Segmentation

Amel Tehami *, Yasmina Teldja Amghar, and Mounia Hendel

Intelligent System Learning and Optimization Team Laboratory of Electrical Engineering and Materials, Higher School in Electrical and Energy Engineering, Oran, Algeria
Email: tehami_amel @ esgee-oran.dz (A.T.); amghar_yasmina @ esgee-oran.dz (Y.T.A.);
hendel_mounia @ esgee-oran.dz (M.H.)
*Corresponding author

***Abstract*—Color image segmentation is a crucial step in various image processing applications, playing a vital role in understanding image content. Nature-inspired optimization algorithms have demonstrated significant potential in enhancing segmentation performance. This paper proposes a novel color image segmentation method based on Wild Horse Optimization (WHO), enhanced with chaos theory, to avoid local optima and accelerate convergence. A logistic map is integrated into the WHO to ensure diverse population initialization and to introduce dynamic perturbations during the optimization process. The proposed method is evaluated on various color images. Metrics such as mean square error, peak signal-to-noise ratio, and structural similarity index are employed to assess the quality of the segmented images. Additionally, the best fitness values, computed using the Davies-Bouldin (DB) index, are analyzed to demonstrate the algorithm's capacity to achieve optimal segmentation solutions. Comparative experiments with other metaheuristic segmentation methods confirm the superior effectiveness of the proposed Logistic Chaos (LC)-based WHO approach.**

***Keywords*—image, logistic map, segmentation, Wild Horse Optimization (WHO)**

I. Introduction

Image segmentation remains a very open research field with unlimited potential. In recent times, a variety of image segmentation schemes have been proposed based on the needs of image understanding and machine vision, including thresholding, edge detection, and region methods [1]. Many methods have been devised to solve the problem of unsupervised segmentation of images. However, they have drawbacks: Great sensitivity to the initial configuration or premature convergence to a local optimum. Consequently, Fan *et al*. [2] have adapted the segmentation problem to an optimization problem.

Nowadays, Artificial Intelligence (AI) is an emerging field that aims to handle the imitation of human intelligence to computers. AI techniques are considered as crucial in technology, contributing in looking for solutions to many challenging problems that different applications in computer science face [3].

Bio inspired algorithms are well-known techniques of AI in solving difficult and combinatorial optimization problems. They are population-based techniques stimulated by behavior in animals. The bio inspired algorithms are combined with image segmentation techniques with the aim to find the optimal parameters required in the segmentation techniques.

Several image segmentation surveys have been published. Yan *et al.* [4] improved the Whale Optimization Algorithm (WOA) based on Kapur to perform multi-level segmentation on hydrological images, and compared the experimental results with algorithms such as bat algorithm, flower polarization algorithm. Zhu *et al.* [5] proposed a multi strategy learning manta ray foraging optimization algorithm. Ewees *et al.* [6] fused the artificial bee colony with the sine cosine algorithm to form an improved algorithm. Duan *et al.* [7] improved the cuckoo search algorithm by parameter adaptive and dynamic weighted random walk strategy. Moreover, Sharma *et al.* [8] recently advanced firefly further by integrating opposition-based learning for faster, more robust Magnetic Resonance Imaging (MRI) color image segmentation.

In recent years, the chaotic functions are mostly used to balance the exploration and exploitation phases in bio inspired algorithms [9]. It can increase convergence speed and diversity in metaheuristic algorithms with chaotic maps. Thus, better results are obtained from these algorithms. Many researchers have added chaos theory to different metaheuristic optimization algorithms to increase the algorithm's ability to obtain the optimum solution [10–13]. Some of the chaos-based bio inspired algorithms for the segmentation. Hosny *et al.* [14] proposed an enhanced version of the coronavirus optimization algorithm for satellite image segmentation. Sajad and Das [15] introduced a novel image segmentation method that combines levy flight, chaos theory, and the gravitational search algorithm.

Li *et al.* [16] introduced an improved image segmentation approach that combines a chaotic initialized chimp optimization algorithm with Cauchy mutation. Zhao *et al*. [17] enhanced the ant colony optimization

Manuscript received September 22, 2025; revised October 15, 2025; accepted November 21, 2025; published March 26, 2026.

algorithm by incorporating a chaotic intensification strategy and random spare/replacement strategy. Bernoulli, tent, quadratic, and logistic maps were adapted to the cuckoo search optimization algorithm [18].

Xu *et al*. [19] introduced a hybrid two-dimensional hyperchaotic system combined with genetic recombination for color image encryption, achieving strong key sensitivity and resistance to differential attacks. Similarly, Lei *et al.* [20] developed a novel fourth-direction hyperchaotic system that exhibits higher complexity and improved diffusion properties in color image encryption. Moreover, Lai and Liu [21] proposed a family of image encryption schemes based on hyperchaotic systems and cellular automata neighborhood, demonstrating that the coupling of cellular automata with hyperchaotic dynamics significantly enhances diffusion and confusion effects.

These recent studies clearly highlight the growing role of chaos-based mechanisms in complex visual data processing. The Wild Horse Optimization (WHO) originally developed to solve complex engineering optimization problems. WHO has been applied to various optimization domains for example, it has been employed in extracting model parameters in photovoltaic systems, solving nonlinear multi-objective optimization problems in energy management and solving link failure problems in underwater channels [22–24]. Although WHO can achieve satisfactory results on some practical issues, there are still some problems, such as a limited exploitation capability and stagnation of locally optimal solutions. Therefore, it is necessary to improve WHO according to practical problems. Ewees *et al.* [25] proposed an improved version of WHO by using the spiral position update strategy of the WOA.

Although WHO has proven effective in various optimization problems, its adoption in image processing, particularly in segmentation, is still relatively scarce in the current literature. Chen *et al*. [26] proposed an improved version of the wild horse optimizer, to address the problem of band selection in hyperspectral images. Maranco *et al.* [27] applied an improved WHO algorithm for skin lesion segmentation. Zhang *et al.* [28] presents an enhancement to the wild horse optimizer for medical image segmentation. The method incorporates chaos initialization to improve the diversity and exploration capabilities of the WHO algorithm. In this study, a novel color image segmentation method is proposed by integrating the Logistic Chaotic map into the WHO (LC-WHO) algorithm to ensure diverse population initialization and introduce dynamic perturbations throughout the optimization process. This approach improves the quality of the initial individuals, offering the advantage of segmenting the image in an optimal way according to the Davies-Bouldin (DB) index used as the objective function.

Image segmentation represents a crucial preprocessing step for subsequent high-level tasks such as object recognition and image classification. The quality of segmentation directly affects the accuracy of extracted features and the performance of classification algorithms. Recent studies have explored various learning-based approaches to enhance classification accuracy. For example, Iqbal *et al.* [29] conducted a comparative investigation of learning algorithms for image classification with small datasets, emphasizing the importance of well-structured image regions for robust learning. Similarly, Iqbal *et al*. [30] proposed a deep learning-based morphological classification of human sperm heads, demonstrating how precise segmentation improves the morphological analysis and classification results. These works highlight the relevance of accurate segmentation, such as that provided by LC-WHO, as a foundation for reliable feature extraction and advanced visual understanding in domains like medical and satellite imaging.

The rest of this paper is organized as follows: Section II formulates the segmentation problem. Section III briefly introduces the chaos theory and logistic map. Section IV introduces an overview of WHO. Section V explains the proposed method and its application in color image segmentation. Subsequently, the experimental results of the proposed method are discussed in Section VI. Finally, the conclusion is presented in Section VII.

II. Formalizing the Segmentation Problem

The segmentation seeks to partition an image I into disjoint subsets and related, called regions R_i. Each region is homogeneous and that the union of two adjacent regions is not homogeneous [1].

Therefore, segmentation is a partition of the image into regions, respecting this definition for $P(.)$, where P is a given predicate (often related to a criterion of homogeneity). From a mathematical point of view, Abdulateef *et al.* [31] defined segmentation S of all pixels in an image I, as an ensemble of regions R_i (i from 1 to n); $S = \{R_1, R_2, .., R_n\}$ as in Eq. (1).

$$\bigcup_{i=1}^{n} R_i = I \tag{1}$$

where $R_i \cap R_j = \{\}$ for $I \neq j$ and $P(R_i)$ = True, $P\left(R_i \cup R_j\right)$ = False (R_i adjacent to R_j).

Segmentation algorithm tries to find a partition R_i such as the similarity between pixels of the same region is maximal and between the pixels of different groups is minimal. From the original image, multiple partitions can be proposed, hence the need to define an objective function which must evaluate a region based on similarity and dissimilarity measures of pixels.

III. Chaos Theory and Logistic Map

Chaos theory describes systems that are non-periodic, unpredictable, and lack specific patterns. One of the most important characteristics of such systems, known as ergodicity, allow the system to exhibit dynamic behavior without repeating within a certain range [32]. Chaotic maps are deterministic systems which are sensitive to

initial conditions and vary according to disordered/random behavior. Most metaheuristic algorithms rely heavily on long-period random number sequences.

However, this reliance can lead to an increased risk of the algorithm becoming trapped in local optima particularly when the generated random numbers cluster in a specific region or repeat. To mitigate this, the generated numbers should be diverse and well-distributed across the search space [33].

Chaos-based approaches address these limitations using chaotic map a class of discretized time systems that exhibit chaotic behavior. These maps produce sequences that are inherently unpredictable and non-periodic [32]. Since chaotic maps generate numbers with non-repetition and ergodicity, improved search can be expected. A chaotic sequence is typically formed from the cumulative effect of chaotic variables applied during each iteration. Incorporating such sequences enhances the algorithm's ability to escape local minima and explore the global search space more effectively.

Consequently, bio inspired algorithms that integrate chaotic maps particularly during the initialization of the random number sequence are expected to develop viable solutions more rapidly and efficiently for complex optimization problems. Although various chaotic maps exist, such as tent, sine, or Henon maps, in this study we have chosen to use the logistic map to introduce chaotic dynamics into the algorithm. The logistic map was adopted as a chaos generator to enhance the exploration capabilities of the WHO algorithm. This map is defined by the following Eq. (2).

$$H_{n+1} = \mu H_n (1 - H_n) \tag{2}$$

where $H \in (0, 1)$ and $\mu \in (3.57, 4)$ are known as control parameters ensuring chaotic behavior.

The logistic map is widely used in chaos-based algorithms due to its simplicity and its ability to produce non-periodic and highly sensitive sequences [34, 35].

IV. Wild Horse Optimization

A new bio inspired algorithm, called Wild Horse Optimization (WHO) algorithm, was proposed to solve optimization problems by mimicking the hierarchy and behavior of horses [36].

The algorithm, which is inspired by the unique mating behavior of wild horses, ensures that individuals within the same family cannot mate with each other. Additionally, the algorithm considers the grazing behavior of horses, where they graze together in the presence of a stallion.

Furthermore, the algorithm incorporates group leadership behavior, with the stallion guiding the group to a more suitable habitat. This includes utilizing the current habitat if the group is dominant or leaving the area if another group holds dominance. Finally, the selection of the stallion is based on its fitness [37].

A. Creating Initial Populations, Horse Groups and Determining Leaders

If N individuals and G groups exist, then the number of non-leaders (mares and foals) is $N–G$, and the number of leaders is G. The proportion of stallions is defined as PS, which is G/N. Then, the fitness of each member of the initial population is calculated and leaders are selected among the group members based on the obtained fitness.

B. Grazing Behavior

As stated previously, most of a foal's life is spent grazing near its group. To simulate the grazing phase, we assume that the stallion position existed in the grazing area center. The following Eq. (3) is used to enable other individuals to move.

$$X_{G,j}^{i} = 2Z\cos(2\pi RZ)(Stallion_j - X_{G,j}^{i}) + Stallion_j \tag{3}$$

where $X_{G,j}^{i}$ and $Stallion_j$ are the positions of the i^{th} group member and *Stallion* in the j^{th} group, respectively. R is a random number between −2 and 2, and Z is an adaptive parameter computed by Eq. (4).

$$\begin{aligned} &P = \overrightarrow{V1} < TDR, IDX = (P == 0), \\ &Z = R1\Theta\, IDX + \overrightarrow{V2}\Theta(\sim IDX) \end{aligned} \tag{4}$$

where P is a vector containing 0 and 1, and its dimension equals the dimension of the problem. $\overrightarrow{V1}$ and $\overrightarrow{V2}$ are random vectors between 0 and 1, and $R1$ is a random number between 0 and 1. TDR is a linearly decreasing parameter computed by Eq. (5).

$$TDR = 1 - \left(\frac{t}{T}\right) \tag{5}$$

where t and T are the current and maximum iterations respectively.

C. Horse Mating Behavior

One of the unique behaviors of horses compared to other animals is separating foals from their original groups prior to their reaching puberty and mating. To be able to simulate the behavior of mating between horses, the following Eq. (6) is used.

$$X_{G,k}^{p} = Crossover(X_{G,i}^{q}, X_{G,j}^{z}) \;\; i \neq j \neq k \tag{6}$$

where $X_{G,k}^{p}$ is the position of horse p in group k, which is formed by positions of horse q in group i and horse z in group j. In the basic WHO, the probability of crossover is set to a constant named PC.

D. Group Leadership

Group leaders will lead other group members to a suitable area (waterhole). Group leaders will also compete for the waterhole, leading the dominant group to employ the waterhole first.

The following Eq. (7) is used to simulate this behavior.

$$Stall_{G,j} = \begin{cases} 2Z\cos(2\pi RZ)(Wh - Stallion_{G,j}) + Wh \ , \ if \ rand > 0.5 \\ 2Z\cos(2\pi RZ)(Wh - Stallion_{G,j}) - Wh \ , \ if \ rand \le 0.5 \end{cases} \quad (7)$$

where $Stall_{G,j}$ and $Stallion_{G,j}$ are the candidate position and the current leader position in the j^{th} group, respectively. Wh is the position of the waterhole.

E. Exchange and Selection of Leaders

At first, leaders are selected randomly. After that, leaders are selected based on their fitness values. To simulate the exchange between leader positions and other individuals, the Eq. (8) is used.

$$Stall_{G,j} = \begin{cases} X^i_{G,j} & if \ fit(X^i_{G,j}) < fit(Stall_{G,j}) \\ Stall_{G,j} & if \ fit(X^i_{G,j}) \ge fit(Stall_{G,j}) \end{cases} \quad (8)$$

where $X^i_{G,j}$ and $Stall_{G,j}$ are the fitness values of foal and stallion, respectively.

V. Proposed Logistic Chaos-Based Wild Horse Optimization

In this study, the WHO, known for its effective performance across various applications, is employed in combination with the logistic chaotic map to enhance its global search capability. The integration of chaos aims to prevent the algorithm from getting trapped in local optima and promotes convergence toward the global optimum. By leveraging the ergodic nature of chaotic system, the search process becomes more diverse and efficient, minimizing the likelihood of revisiting the same positions in the search space.

The main step of Logistic Chaos-based Wild Horse Optimization (LC-WHO) can be summarized as follows.

A. Creating Initial Populations and Calculating the Fitness Values

WHO uses the rand function to randomly initialize the population, resulting in a high randomness but uneven distribution across the entire solution space, which results in a sluggish population search speed, poor diversity and low solution accuracy. To address these issues, we integrate the logistic sequence to map the initialized populations.

The calculation method of logistic chaotic map is given in Eq. (2). After the initial population generated by logistic chaotic map, several N solutions are obtained. Then, the fitness of each member of the initial population is calculated and leaders are selected among the group members based on the obtained fitness.

In the Logistic Chaos-based Wild Horse Optimization (LC-WHO) algorithm, the Davies-Bouldin (DB) index is employed as the objective function and is evaluated according to Eq. (9) [38].

$$DB = \frac{1}{K}\sum_{i=1}^{K} \max_{i \ne j} \left\{ \frac{S_i + S_j}{d(C_i, C_j)} \right\} \quad (9)$$

where K denotes the number of regions. $d(C_i, C_j)$ denotes the distance between the centroids of regions i and j. S_i is the average distance between the region's center and all its pixels, which is defined as Eq. (10).

$$S_i = \frac{1}{n_i}\sum_{j=1}^{n_i} d(y_j - C_i) \quad (10)$$

The smallest value of the DB index indicates the optimal partition, representing more effective and well-separated segmentation.

After the generation of the initial population, each pixel is defined by the three dimensions of the RGB color space and assigned to the class whose center is the nearest. All horses are then evaluated using the fitness function.

The segmentation is therefore performed in the RGB color space, which directly represents the image's native pixel intensities without requiring nonlinear transformations. Although perceptual spaces such as lab or HSV can sometimes provide better alignment with human vision, RGB was selected for its simplicity and its compatibility with the Davies-Bouldin index, which effectively evaluates the compactness and separation of color clusters in this 3D space.

B. Position Updating Strategy Integration in Grazing Behavior

The position of each horse during the grazing behavior is modulated using a chaotic value generated by the logistic map.

This post-update adjustment introduces dynamic perturbation, encouraging broader search and preventing premature convergence. The new position of horse is given by Eq. (11).

$$X^i_{G,j} = H(2Z\cos(2\pi RZ)(Stallion_j - X^i_{G,j}) + Stallion_j) \quad (11)$$

where H is the chaotic value derived from the logistic map as shown in Eq. (2).

C. Simulation of Mating Behavior Using the Logistic Map

To enhance the exploration capabilities of the algorithm, the mating behavior is modified by incorporating chaotic dynamics from the logistic map. The crossover operation, which generates new horse from two parent solutions, plays a crucial role in maintaining

diversity within the population. A chaotic factor H is introduced to regulate the contribution of each parent dynamically. The chaotic crossover is defined in Eq. (12).

$$Crossover(X_{G,i}^{q}, X_{G,j}^{z}) = \frac{HX_{G,i}^{q} + (1-H)X_{G,j}^{z}}{2} \quad (12)$$

D. Updating the Stallion Position and Davies-Bouldin Index

The competitive behavior among groups is modeled by Eq. (7). Each group is directed toward the waterhole by its respective leader. In the context of color image segmentation, the waterhole symbolizes the best partition found during the current iteration, guiding the search toward more promising segmentation results.

To improve the exploration and make the movement of the groups more dynamic, the logistic chaotic map is used to help the algorithm avoid being trapped in local solutions and encourages it to explore more diverse regions in the search space. The new position of Stallion is given by Eq. (13).

$$Stall_{G,j} = \begin{cases} H(2Z\cos(2\pi RZ)(Wh - Stallion_{G,j}) + Wh) & if\ rand > 0.5 \\ H(2Z\cos(2\pi RZ)(Wh - Stallion_{G,j}) - Wh) & if\ rand \le 0.5 \end{cases} \quad (13)$$

The stallion is selected based on its fitness value (DB index). If a group member has a better fitness value than the current leader, the leader's position is updated and replaced by that of the better-performing member. This behavior is modeled by the following Eq. (14).

$$Stall_{G,j}^{new} = \begin{cases} X_{G,j}^{new} & if\ DB(X_{G,j}^{new}) < DB(Stall_{G,j}^{new}) \\ Stall_{G,j}^{new} & if\ DB(X_{G,j}^{new}) \ge DB(Stall_{G,j}^{new}) \end{cases} \quad (14)$$

In LC-WHO, foals and stallions have a more flexible method to update their positions.

The logistic map helps search agents achieve a better balance between exploration and exploitation, obtain high-quality solutions and improve the convergence speed.

The pseudocode of LC-WHO is shown in algorithm.

Algorithm: Pseudocode of LC-WHO

Set the color image to be segmented
Set population size N, the maximum number of iterations T_2, the number of iteration for each group T_1, PC value and μ logistic parameter
Initialize the population generated using Logistic map and calculate the fitness using Eq. (9)
While the end criterion is not satisfied ($t \le T_2$)
Create foal groups and select stallions
While the end criterion is not satisfied ($t_1 \le T_1$)
Calculate TDR using Eq. (5)
Calculate Z using Eq. (4)
For the number of stallions
  For the number of foals
   If rand>PC **then**
    Update the position of the foal by Eq. (11)
   Else
    Update the position of the foal by Eq. (12)
   End if
  End for
 Generate the position of stallion by Eq. (13)
 If the candidate position of the stallion is better
 Replace the position of the stallion by the candidate position using Eq. (14)
 End if
 End for
 End while for each group (if the number of maximal iteration T_1 is reached)
 The different groups are combined to form again the population of Horses
 End While (if the number of maximal iteration T_2 is reached)
Segmented the image with the best solution

VI. Result and Discussion

To verify the practicality of LC-WHO in the field of color image segmentation, three test images were selected and resized to 256×256 pixels to analyze the algorithm's segmentation effects presented in Figs. 1–3.

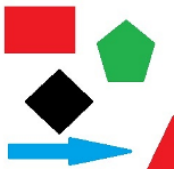

Fig. 1. Image test 1.

Fig. 2. Image test 2.

Fig. 3. Image test 3.

Additionally, three Landsat-derived satellite images Figs. 4–6 were freely obtained online and used at their original resolutions to assess LC-WHO's performance on real-world remote sensing. To evaluate the performance of the proposed LC-WHO algorithm, three types of studies will be conducted. First is a comparative study with classical bio-inspired methods. Second is a comparative study with WOA variants based on chaos theory. Third, the impact of the chaotic parameter μ in the logistic map will be analyzed to determine its influence on the exploration capabilities and overall performance of the LC-WHO algorithm.

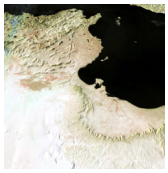

Fig. 4. Image sat 1.

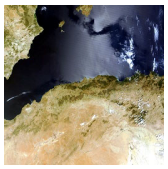

Fig. 5. Image sat 2.

Fig. 6. Image sat 3.

A. Comparative Analysis with Bio Inspired Methods

The effectiveness of the proposed LC-WHO algorithm is assessed through a comparative study with other well-known bio-inspired optimization methods that do not incorporate chaotic strategies. Specifically, the comparison includes the classical Particle Swarm Optimization (PSO) [39, 40], the Shuffled Frog-Leaping Algorithm (SFLA) [41, 42], and the standard WHO [43] without chaotic enhancement. The experimental environment runs on Windows 10 (64-bit) with Intel core i7 microprocessor, 32 GB RAM and the JAVA programming language (NetBeans IDE 7.4).

The experimental parameter values of LC-WHO determined after several tests and ensuring good convergence are shown in Table I.

TABLE I. INITIAL PARAMETERS OF LC-WHO

Parameter	Description	Value
N	Population size	60
G	Number of groups	10
T_1	Number of iterations (local search)	50
T_2	Number of iterations (global search)	150
PC	Crossover parameter	0.13
μ	Logistic chaos parameter	4.00

The effectiveness and feasibility of the LC-WHO are verified by comparing it with other algorithms. The corresponding experimental results for the comparative algorithms on the test images are presented in the subsequent Figs. 7–9.

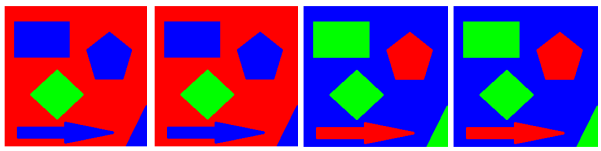

Fig. 7. Image test 1 segmentation using PSO, SFLA, WHO and LC-WHO (respectively from left to right).

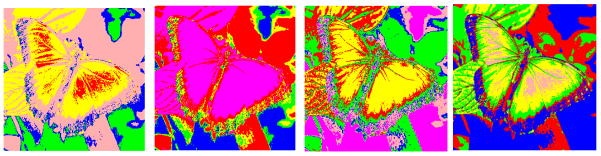

Fig. 8. Image test 2 segmentation using PSO, SFLA, WHO and LC-WHO (respectively from left to right).

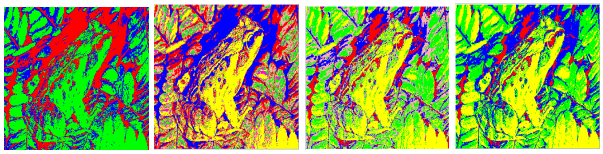

Fig. 9. Image test 3 segmentation using PSO, SFLA, WHO and LC-WHO (respectively from left to right).

To evaluate the quality of segmented images, five important indicators are used to estimate the image segmentation effect of different algorithms as follows.

1) Fitness value

The fitness value reflects the segmentation accuracy of each algorithm. In this work, the Davies-Bouldin (DB) index is employed as the objective function and is calculated using Eq. (9).

2) Run time

The algorithm consumes less time, which means that the algorithm has a faster calculation process.

3) Mean Squared Error (MSE)

The MSE quantifies the average squared difference between corresponding pixels of the original image and the segmented image detected as Eq. (15) [44].

$$MSE = \frac{1}{MN}\sum_{i=1}^{m}\sum_{j=1}^{n}\left[I(i,j) - SE(i,j)\right]^2 \tag{15}$$

where I and SE denote the original and segmented images, which have dimensions $M \times N$, respectively. The lower value of MSE indicates the optimal performance of the segmentation algorithms.

4) Peak Signal-to-Noise Ratio (PSNR)

The PSNR is a measure used to assess the difference between a reference image and a segmented image and it relies on the intensity values, which is calculated as Eq. (16) [44, 45].

$$PSNR = 10\log_{10}\left[\frac{\max^2}{MSE}\right] \tag{16}$$

The maximum variation in the source image data is denoted by max. A higher PSNR value indicates better performance of the segmentation algorithm, reflecting greater similarity between the original and segmented images.

5) Structure Similarity Index (SSIM)

The SSIM is a similarity measure between the provided image and the segmented image [46]. If the SSIM is close to 1, then the image segmentation result is

better. The SSIM is described as Eq. (17).

$$SSIM(I,SE)=\frac{(2\mu_I\mu_{SE}+C_1)(2\sigma_{I,SE}+C_2)}{(\mu_I^2+\mu_{SE}^2+C_1)(\sigma_I^2+\sigma_{SE}^2+C_2)} \quad (17)$$

where μ_I and μ_{SE} refer to the mean intensity of I and SE respectively, while σ_I and σ_{SE} refer to the standard deviation of I and SE, respectively. σ_I and σ_{SE} represent a variance of I and SE. C_1 and C_2 are constants. The maximum value of SSIM refers to a better performance.

The Figs. 10–12 illustrate the segmentation results of satellite images obtained using the proposed LC-WHO algorithm in comparison with different Bio inspired approaches, including PSO, SFLA, and WHO.

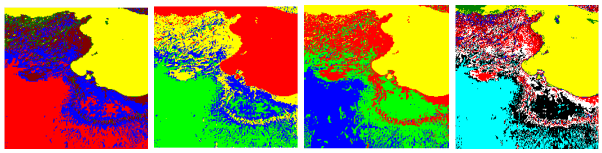

Fig. 10. Image sat 1 segmentation using PSO, SFLA, WHO and LC-WHO (respectively from left to right).

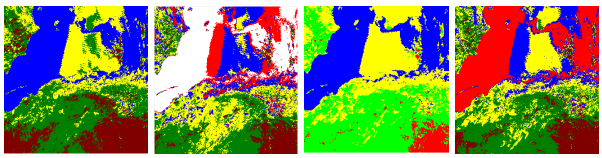

Fig. 11. Image sat 2 segmentation using PSO, SFLA, WHO and LC-WHO (respectively from left to right).

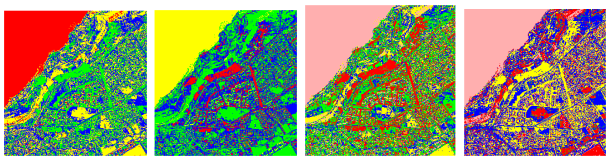

Fig. 12. Image sat 3 segmentation using PSO, SFLA, WHO and LC-WHO (respectively from left to right).

From the visual segmentation results illustrated in the all figures, it can be observed that all four algorithms PSO, SFLA, WHO, and the proposed LC-WHO produce satisfactory segmentations. However, the images segmented by LC-WHO exhibit slightly superior visual quality, with clearer object boundaries and better preservation of structural details. The differences are subtle, but LC-WHO consistently achieves more refined segmentation across the images.

From the visual segmentation results illustrated in the all figures, it can be observed that all four algorithms PSO, SFLA, WHO, and the proposed LC-WHO produce satisfactory segmentations. However, the images segmented by LC-WHO exhibit slightly superior visual quality, with clearer object boundaries and better preservation of structural details. The differences are subtle, but LC-WHO consistently achieves more refined segmentation across the images.

The numerical results presented in Tables II and III highlight the comparative performance of PSO, SFLA, WHO, and the proposed LC-WHO algorithm on tests images and satellite images uses five metrics: Run time, DB-Index, MSE, PSNR, and SSIM.

TABLE II. COMPARATIVE PERFORMANCE OF DIFFERENT ALGORITHMS ON TEST IMAGES

Algorithms	Images	Run Time (ms)	DB-Index	MSE	PSNR	SSIM
PSO	Test 1	3113	0.776	106.87	27.12	0.689
	Test 2	5895	0.864	82.57	28.74	0.775
	Test 3	5581	0.835	85.77	28.53	0.793
SFLA	Test 1	3102	0.772	106.28	27.85	0.755
	Test 2	5925	0.872	82.04	28.82	0.780
	Test 3	5479	0.821	85.65	28.38	0.795
WHO	Test 1	3025	0.768	101.06	28.78	0.787
	Test 2	5627	0.869	79.52	28.92	0.797
	Test 3	5466	0.815	74.17	30.28	0.808
LC-WHO	Test 1	3019	0.754	101.04	28.91	0.790
	Test 2	5644	0.861	69.45	29.98	0.810
	Test 3	5437	0.810	72.05	31.12	0.821

TABLE III. COMPARATIVE PERFORMANCE OF DIFFERENT ALGORITHMS ON SATELLITES IMAGES

Algorithms	Images	Run Time (ms)	DB-Index	MSE	PSNR	SSIM
PSO	Sat 1	4102	0.741	57.18	32.05	0.886
	Sat 2	5227	0.657	60.54	30.94	0.865
	Sat 3	6582	0.638	50.12	34.89	0.901
SFLA	Sat 1	4025	0.735	55.98	32.03	0.897
	Sat 2	5224	0.652	60.21	30.97	0.875
	Sat 3	5928	0.628	50.07	34.94	0.908
WHO	Sat 1	4024	0.725	51.43	32.10	0.902
	Sat 2	5117	0.708	63.09	29.86	0.814
	Sat 3	5857	0.541	47.65	35.18	0.912
LC-WHO	Sat 1	4018	0.702	48.35	32.79	0.920
	Sat 2	5119	0.593	59.11	31.81	0.894
	Sat 3	5854	0.498	44.28	35.34	0.920

The performance of the proposed LC-WHO algorithm was evaluated on six images and compared with PSO, SFLA, and standard WHO. As shown in Tables II and III, LC-WHO consistently achieves superior results across all evaluation metrics. Specifically, in satellites images it attains the lowest DB index values (0.702, 0.593, 0.498), indicating more compact and well-separated segments. In terms of MSE, LC-WHO produces smaller errors (48.35, 59.11, 44.28), demonstrating that the segmented images are closer to the originals. PSNR values are also higher (32.79, 31.81, 35.34), confirming better reconstruction fidelity. Regarding SSIM, LC-WHO achieves the highest scores (0.920 for sat 1 and sat 3, 0.894 for sat 2), reflecting improved perceptual quality and structural similarity.

Additionally, LC-WHO maintains competitive run times (4018 ms, 5119 ms, 5854 ms), which are comparable or slightly faster than the other methods, showing that enhanced segmentation performance does not come at the expense of computational efficiency.

Overall, these quantitative results confirm that LC-WHO provides the best balance between segmentation accuracy, visual quality, and efficiency. The improvements are attributed to the incorporation of chaotic dynamics via the logistic map, which enhances the exploration and exploitation capabilities of the standard WHO algorithm.

B. Comparative Study with Chaos Based Whale Optimization Algorithm

The WOA is a recently developed meta-heuristic inspired by the hunting behavior of humpback whales. Like other meta-heuristics, WOA can suffer from slow convergence, limiting its performance on complex problems [47]. To improve global convergence and solution quality, chaos theory can be incorporated into WOA. In particular, the logistic map is used in LC-WOA to tune its main parameters, effectively balancing exploration and exploitation [48].

The primary claim of this work is the superior effectiveness of the logistic chaos-based enhancement. To validate this, the proposed LC-WHO algorithm is compared with a competitive, chaos-enhanced metaheuristic named LC-WOA. Both algorithms exploit the logistic chaotic map to improve global exploration and avoid premature convergence, providing a fair and rigorous evaluation for color image segmentation tasks.

To ensure a fair comparison, the parameters of both LC-WHO and LC-WOA were initialized according to the values presented respectively in Tables IV and V.

TABLE IV. PARAMETERS OF LC-WHO

Parameter	Description	Value
N	Population size of horses	40
G	Number of groups	10
T_1	Number of iterations (local search)	100
T_2	Number of iterations (global search)	200
PC	Crossover parameter	0.13
μ	Logistic chaos parameter	4.00

TABLE V. PARAMETERS OF LC-WOA

Parameter	Description	Value
N	Population size of whales	40
μ	Logistic chaos parameter	4.00
T_1	Number of iterations (local search)	100
T_2	Number of iterations (global search)	200

The experimental results of the comparative algorithms applied to the satellite images shown in Figs. 4 and 5 are presented in Figs. 13 and 14. These figures illustrate the segmentation performance of each algorithm, allowing a clear visual comparison.

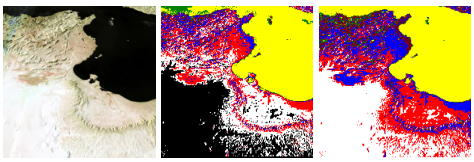

Fig. 13. Image sat 1 segmentation using LC-WHO and LC-WOA (respectively from left to right).

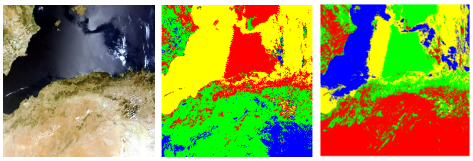

Fig. 14. Image sat 2 segmentation using LC-WHO and LC-WOA (respectively from left to right).

The quantitative outcomes reported in Table VI demonstrate the performance comparison between the LC-WOA and the proposed LC-WHO algorithms applied to satellite images. The evaluation conducted using five objective criteria run time, DB-index, MSE, PSNR, and SSIM.

TABLE VI. COMPARATIVE PERFORMANCE OF LC-WHO AND LC-WOA ON SATELLITES IMAGES

Methods	Images	Run Time (ms)	DB-Index	MSE	PSNR	SSIM
LC-WHO	Sat 1	4014	0.706	48.40	33.02	0.908
	Sat 2	5108	0.588	59.11	31.58	0.900
LC-WOA	Sat 1	4102	0.711	48.43	32.78	0.904
	Sat 2	5114	0.602	59.18	31.30	0.898

The obtained results show that both methods yield very close values across all evaluation metric run time, DB-Index, MSE, PSNR, and SSIM. For sat 1, LC-WHO obtained a DB-Index of 0.706, MSE of 48.40, PSNR of 33.02 dB, and SSIM of 0.908, while LC-WOA achieved 0.711, 48.43, 32.78, and 0.904, respectively. Similarly, for sat 2, LC-WHO reached a DB-Index of 0.588, MSE of 59.11, PSNR of 31.58 dB, and SSIM of 0.900, compared to 0.602, 59.18, 31.30 dB, and 0.898 for LC-WOA. This similarity in performance confirms the beneficial effect of introducing chaotic mapping in both algorithms, which enhances their convergence behavior

and segmentation stability while maintaining competitive accuracy.

C. The Impact of the Chaotic Parameter μ in the Logistic Map

To further investigate the influence of the chaotic mechanism on the performance of the proposed LC-WHO algorithm, an additional experiment was conducted to analyze the impact of the chaotic control parameter μ in the logistic map. Since the value of μ determines the dynamic behavior of the chaotic sequence, it directly affects the balance between exploration and exploitation during the optimization process. Therefore, several values of μ (Table VII) were tested to examine how this parameter influences the convergence speed, exploration capability, and overall segmentation performance of LC-WHO.

TABLE VII. DIFFERENT VALUES OF μ

Parameter	Values
μ	3.57, 3.95, 3.99, 4

In this experiment, the initial parameters of the LC-WHO algorithm (listed in Table VIII) were applied, and image test 1 was used to assess the performance of the method.

TABLE VIII. LC-WHO PARAMETERS

Parameter	Description	Value
N	Population size of horses	80
G	Number of groups	8
T_1	Number of iterations (local search)	250
T_2	Number of iterations (global search)	150
PC	Crossover parameter	0.13

Fig. 15 presents the segmentation results of image test 1 achieved by the proposed LC-WHO algorithm for different values of the chaotic control parameter μ highlighting the influence of this parameter on the quality of the segmentation results.

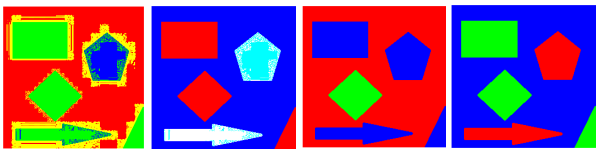

Fig. 15. Image test 1 segmentation with μ = 3.57, 3.95, 3.99 and 4 (respectively from left to right).

The following Table IX summarizes the numerical values corresponding to the different settings of the chaotic parameter μ.

TABLE IX. NUMERICAL RESULTS FOR DIFFERENT VALUES OF THE CHAOTIC PARAMETER

μ	Run Time (ms)	DB-Index	MSE	PSNR	SSIM
3.57	4658	0.941	128.48	20.36	0.641
3.95	4624	0.859	112.87	25.07	0.629
3.99	4625	0.790	104.22	28.55	0.758
4	4622	0.781	104.10	28.87	0.771

D. Results

The results reveal that the choice of μ significantly affects the segmentation quality. When μ increases from 3.57 to 4.00, the DB-Index progressively decreases from 0.941 to 0.781, indicating improved compactness and separation of clusters. At the same time, the PSNR rises from 20.36 dB to 28.87 dB and the SSIM from 0.641 to 0.771, showing better image reconstruction quality and structural consistency. Moreover, the MSE values consistently decrease, confirming that a higher chaotic intensity μ = 4 enhances the balance between exploration and exploitation, leading to more accurate and stable segmentation outcomes.

VII. CONCLUSION

Bio inspired algorithms have demonstrated significant potential in image segmentation due to their capability to effectively explore complex and nonlinear search spaces. In this paper, we introduced LC-WHO, a chaos-enhanced variant of the WHO, which integrates a logistic map to improve the exploration abilities of the population. Specifically, the logistic chaotic map is used to enhance the random initialization strategy of WHO. This not only increases the diversity of the initial population but also reduces the risk of premature convergence and entrapment in local optima.

The proposed LC-WHO algorithm consistently outperformed other methods across multiple evaluation metrics, including DB-Index, MSE, PSNR, SSIM, and run time. These results confirm the benefits of incorporating chaos theory into bio-inspired optimization techniques and establish LC-WHO as a promising and efficient approach for achieving accurate and high-quality of color image segmentation. In future work, we plan to further investigate the influence of different chaotic integration strategies within the WHO framework, including the use of chaotic initialization alone or in combination with chaotic grazing and stallion movement, as well as the application of other chaotic maps such as tent or sine, to confirm the robustness and generality of the proposed LC-WHO model.

CONFLICT OF INTEREST

The authors declare no conflict of interest.

AUTHOR CONTRIBUTIONS

Amel Tehami conceived the main idea of the research, designed the methodology, performed the formal analysis and algorithm implementation, carried out software development, supervised the overall research process, validated the experimental results, and prepared the original draft of the manuscript. Yasmina Teldja Amghar contributed to conceptualization and methodology, participated in data collection and preprocessing conducted part of the investigation and analysis. Mounia Hendel contributed to methodology refinement and played an important role in manuscript revision. All

authors reviewed the results and had approved the final version of the manuscript.

REFERENCES

[1] S. K. Abdulateef and M. D. Salman, "A comprehensive review of image segmentation techniques," *Iraqi Journal for Electrical and Electronic Engineering,* vol. 17, no. 2, pp. 166–175, 2021.

[2] F. Fan, G. Liu, J. Geng, H. Zhao, and G. Liu, "Optimization of remote sensing image segmentation by a customized parallel sine cosine algorithm based on the Taguchi method," *Remote Sensing.* vol. 14, no. 19, 4875, 2022. http://doi.org/10.3390/rs14194875

[3] S. Larabi-Marie-Sainte, R. Alskireen, and S. Alhalawani, "Emerging applications of bio-inspired algorithms in image segmentation," *Electronics*, vol. 10, no. 24, pp. 3116–3130, 2021. https://doi.org/10.3390/electronics10243116

[4] Z. Yan, J. Zhang, Z. Yang, and J. Tang, "Kapur's entropy for underwater multilevel thresholding image segmentation based on whale optimization algorithm," *IEEE Access*, vol. 9. pp. 41294–41319, 2021. http://doi.org/10.1109/ACCESS.2021.3052807

[5] D. Zhu, C. Zhou, Y. Qiu, Y. Tang, and S. Yan, "Kapur's entropy underwater image segmentation based on multi-strategy manta ray foraging optimization," *Multimedia Tools and Applications*, vol. 89, no. 14, pp. 21825–21863, 2023. https://doi.org/10.1007/s11042-022-14024-2

[6] A. A. Ewees, M. A. Elaziz, M. A. A. Al-Qaness, H. A. Khalil, and S. Kim, "Improved artificial bee colony using sine-cosine algorithm for multi-level thresholding image segmentation," *IEEE Access*, vol. 8, pp. 26304–26315, 2020. https://doi.org/10.1109/ACCESS.2020.2971249

[7] L. Duan, S. Yang, and D. Zhang, "Multilevel thresholding using an improved cuckoo search algorithm for image segmentation," *Journal of Supercomputing*, vol. 77, no. 7, pp. 6734–6753, 2021. https://doi.org/10.1007/s11227-020-03566-7

[8] A. Sharma, R. Chaturvedi, and A. Bhargava, "A novel opposition based improved firefly algorithm for multilevel image segmentation," *Multimedia Tools and Applications*, vol. 81, no. 11, pp. 15521–15544, 2022. https://doi.org/10.1007/s11042-022-12303-6

[9] D. Dhawale, V. K. Kamboj, and P. Anand, "An improved chaotic Harris Hawks optimizer for solving numerical and engineering optimization problems," *Engineering with Computers*, vol. 39, no. 2, pp. 1183–1228, 2023. https://doi.org/10.1007/s00366-021-01487-4

[10] W. Zhao, Y. Liu, J. Li, T. Zhu, K. Zhao, and K. Hu, "A wild horse optimization algorithm with chaotic inertia weights and its application in linear antenna array synthesis," *PLOS ONE, vol.* 19, no. 7, e0304971, 2024. doi.org/10.1371/journal.pone.0304971

[11] D. Dhawale, V. K. Kamboj, and P. Anand, "An effective solution to numerical and multi-disciplinary design optimization problems using chaotic slime mold algorithm," *Engineering with Computers*, vol. 38, no. 4, pp. 2739–2777, 2021. https://doi.org/10.1007/s00366-021-01409-4

[12] M. Peng, X. Wei, and H. Huang, "A chaotic adaptive butterfly optimization algorithm," *Evolutionary Intelligence*, vol. 17, no. 1, pp. 493–511, 2024. https://doi.org/10.1007/s12065-023-00832-4

[13] F. A. Özbay, "A modified seahorse optimization algorithm based on chaotic maps for solving global optimization and engineering problems," *Engineering Science and Technology, an International Journal*, vol. 41, 101408, 2023. https://doi.org/10.1016/j.jestch.2023.101408

[14] K. M. Hosny, A. M. Khalid, H. M. Hamza, and S. Mirjalili, "Multilevel thresholding satellite image segmentation using chaotic coronavirus optimization algorithm with hybrid fitness function," *Neural Computing and Applications*, vol. 35, no. 1, pp. 855–886, 2023. https://doi.org/10.1007/s00521-022-07718-z

[15] S. A. Rather and S. Das, "Levy flight and chaos theory-based gravitational search algorithm for image segmentation," *Mathematics*, vol. 11, no. 18, p. 3913, 2023. https://doi.org/10.3390/math11183913

[16] S. Li, Z. Li, W. Cheng, C. Qi, and L. Li, "Multi-level image segmentation combining chaotic initialized chimp optimization algorithm and Cauchy mutation," *Computers, Materials & Continua*, vol. 80, no. 2, pp. 2049–2063, 2024. https://doi.org/10.32604/cmc.2024.051928

[17] D. Zhao, L. Liu, F. Yu *et al*., "Chaotic random spare ant colony optimization for multi-threshold image segmentation of 2D Kapur entropy," *Knowledge-Based Systems*, vol. 216, 106510, 2021. https://doi.org/10.1016/j.knosys.2020.106510

[18] S. Chakraborty and K. Mali, "A multilevel biomedical image thresholding approach using the chaotic modified cuckoo search," *Soft Computing*, vol. 28, no. 6, pp. 5359–5436, 2024. https://doi.org/10.1007/s00500-023-09283-6

[19] Y. Xu, J. Liu, Z. You, and T. Zhang, "A novel color image encryption algorithm based on hybrid two-dimensional hyperchaos and genetic recombination," *Mathematics*, vol. 12, no. 22, 3457, 2024. https://doi: 10.3390/math12223457

[20] J. Lei, X. Zhang, H. Wang, and Y. Li, "Color image encryption based on a novel fourth-direction hyperchaotic system," *Electronics*, vol. 13, no. 12, 2229, 2024. https://doi:10.3390/electronics13122229

[21] Q. Lai and Y. Liu, "A family of image encryption schemes based on hyperchaotic system and cellular automata neighborhood," *Sci. China Technol. Sci.*, vol. 68. no. 3, pp. 1–13, 2025. https:// doi: 10.1007/s11431-024-2678-7

[22] A. Ramadan, S. Kamel, I. B. M. Taha, and M. Tostado-Véliz, "Parameter estimation of modified double-diode and triple-diode photovoltaic models based on wild horse optimizer," *Electronics*, vol. 10, no. 18, 2308, 2021. https://doi.org/10.3390/electronics10182308

[23] M. Milovanović, D. Klimenta, M. Panić, J. Klimenta, and B. Perović, "An application of wild horse optimizer to multi-objective energy management in a micro-grid," *Electrical Engineering*, vol. 104, no. 6, pp. 4521–4541, 2022. https://doi.org/10.1007/s00202-022-01636-y

[24] S. Saha and R. Arya, "Improved hybrid node localization using the Wild Horse Optimization in the underwater environment," *International Journal of System Assurance Engineering and Management*, vol. 14. pp. 865–885, 2023. https://doi.org/10.1007/s13198-021-01388-1

[25] A. A. Ewees, F. H. Ismail, and R. M. Ghoniem, "Wild horse optimizer-based spiral updating for feature selection," *IEEE Access*, vol. 10. pp. 106258–106274, 2022. doi: 10.1109/ACCESS.2022.3211263

[26] T. Chen, Y. Sun, H. Chen, and W. Deng, "Enhanced wild horse optimizer with Cauchy mutation and dynamic random search for hyperspectral image band selection," *Electronics*, vol. 13, no. 10, 1930, 2024. https:// doi.org/10.3390/electronics13101930

[27] M. Maranco, A. K. Tyagi, and S. Murugaiyan, "Improved wild horse optimizer with deep learning model for skin lesion detection and classification on dermoscopic images," in *Proc. International Conference on Intelligent Systems Design and Applications,* 2023, pp. 414–424.

[28] L. Zhang, M. Qinghe Li, and S. Li, "Application of improved wild horse optimizer based on chaos initialization in medical image segmentation," in *Proc. 13th Int. Conf. Computer Engineering and Networks*, 2024, vol. 1125, pp. 334–343.

[29] I. Iqbal, G.A.Odesanmi, J. Wang and L. Liu, "Comparative investigation of learning algorithms for image classification with small dataset," *Appl. Artificial Intelligence*, vol. 35, no. 10, pp. 697–716, 2021. https://doi.org/10.1080/08839514.2021.1922841

[30] I. Iqbal, G. Mustafa, and J. Ma, "Deep learning-based morphological classification of human sperm heads," *Diagnostics*, vol. 10, no. 5, p. 325, 2020. https://doi.org/10.3390/diagnostics10050325

[31] S. K. Abdulateef, S. R. A. Ahmed, and M. D. Salman, "A novel food image segmentation based on homogeneity test of K-means clustering," in *Proc. IOP Conference Series: Materials Science and Engineering*, vol. 928, no. 3, 2020, 032059. https://doi.org/10.1088/1757-899X/928/3/032059

[32] F. Serbet and T. Kaya, "New comparative approach to multi-level thresholding: Chaotically initialized adaptive meta-heuristic optimization methods," *Neural Computing and Applications*, vol. 37, no. 14, pp. 8371–8396, 2025. https://doi.org/10.1007/s00521-025-11016-9

[33] E. A. Zaimoğlu, N. Yurtay, H. Demirci, and Y. Yurtay, "A binary chaotic horse herd optimization algorithm for feature selection," *Engineering Science and Technologyan International Journal*, vol. 44, 101453, 2023. https://doi.org/10.1016/j.jestch.2023.101453

[34] E. A. Zaimoğlu, N. Yurtay, H. Demirci, and Y. Yurtay, "A binary chaotic horse herd optimization algorithm for feature selection,"

Engineering Science and Technologyan International Journal, vol. 44, 101453, 2023. https://doi.org/10.1016/j.jestch.2023.101453

[35] J. Rajpurohit, T. K. Sharma, A. Sharma, and S. Bhushan, "A modified honey badger algorithm with logistic map and enhanced exploitation," in *Proc. International Conference on Soft Computing: Theories and Applications*, 2023, pp. 435–446.

[36] I. Naruei and F. Keynia, "Wild horse optimizer: A new meta-heuristic algorithm for solving engineering optimization problems," *Engineering with Computers*, vol. 38, pp. 3025–3056, 2022. https://doi.org/10.1007/s00366-021-01438-z

[37] R. Zheng, A. G. Hussien, H. M. Jia, L. Abualigah, S. Wang, and D. Wu, "An improved wild horse optimizer for solving optimization problems," *Mathematics*, vol. 10, no. 8, p. 1311, 2022. https://doi.org/10.3390/math10081311

[38] F. Ros, R. Riad, and S. Guillaume, "PDBI: A partitioning Davies-Bouldin index for clustering evaluation," *Neurocomputing*, vol. 528, pp.178–199, 2023.

[39] S. Sheoran, N. Mittal, and A. Gelbukh, "Change detection in remote-sensed data by particle swarm optimized edge detection image segmentation technique," in *Proc. 2020 Int. Conf. Comput. Intell. Data Sci*., 2020, pp. 809–817.

[40] S. Sheoran, N. Mittal, and A. Gelbukh, "Hybrid change detection technique with particle swarm optimization for land use land cover using remote-sensed data," in *Proc. Int. Conf. Comput. Intell. Data Sci*., 2024, pp. 411–420. https://doi.org/10.1007/978-981-99-6544-1_31

[41] A. Tehami and H. Fizazi, "Unsupervised segmentation of images based on shuffled frog-leaping algorithm," *Journal of Information Processin25g Systems*, vol. 13, no. 2, pp. 370–384, 2017, https://doi.org/10.3745/JIPS.02.0055

[42] V. D. Gopal, G. Shreedevi, and A. Geetha, "Image segmentation recommender using bio-inspired algorithms," *SSRG International Journal of Electronics and Communication Engineering*, vol. 11, no. 5, pp. 262–275, 2024. https://doi.org/10.14445/23488549/IJECE-V11I5P125

[43] A. Tehami and Y. T. Amghar, "Wild horse optimization for satellite images segmentation," in *Proc. IEEE Mediterranean and Middle-East Geoscience and Remote Sensing Symposium*, 2024, pp. 159–163. doi: 10.1109/M2GARSS57310.2024.10537265

[44] A. Makandar, S. Kaman, R. Biradar, and S. B. Javeriya, "Impact of edge detection algorithms on different types of images using PSNR and MSE," *LC International Journal of STEM*, vol. 3, no. 4, pp. 1–11, 2022. https://doi.org/10.5281/zenodo.7607059

[45] L. Abualigah, N. K. Al-Okbi, S. A. Alomari *et al.,* "Optimized image segmentation using an improved reptile search algorithm with Gbest operator for multi-level thresholding," *Scientific Reports*, vol. 15, no. 1, 12713, 2025. https://doi.org/10.1038/s41598-025-96429-1

[46] I. Bakurov, M. Buzzelli, R. Schettini, M. Castelli, and L. Vanneschi, "Structural Similarity Index (SSIM) revisited: A data-driven approach," *Expert Systems with Applications*, vol. 189, 116087, 2022. https://doi.org/10.1016/j.eswa.2021.116087

[47] G. Kaur and S. Arora, "Chaotic whale optimization algorithm," *Journal of Computational Design and Engineering*, vol. 5, no. 3, pp. 275–284, 2018. https://doi.org/ 10.1016/j.jcde.2017.12.006

[48] J. Liu, J. Tan and B. Xu, "An image segmentation method based on improved whale optimization algorithm," in *Proc. SPIE 13646, International Conference on Pattern Recognition and Image Analysis (PRIA 2024)*, 2025, vol. 13646, pp. 245–251.